

Fabrication of Ultrathin Membrane via Layer-by-Layer Self-assembly Driven by Hydrophobic Interaction Towards High Separation Performance

Jing Zhao,^{†,‡} Fusheng Pan,^{†,‡} Pan Li,^{†,‡} Cuihong Zhao,^{†,‡} Zhongyi Jiang,^{*,†,‡} Peng Zhang,[§] and Xingzhong Cao[§]

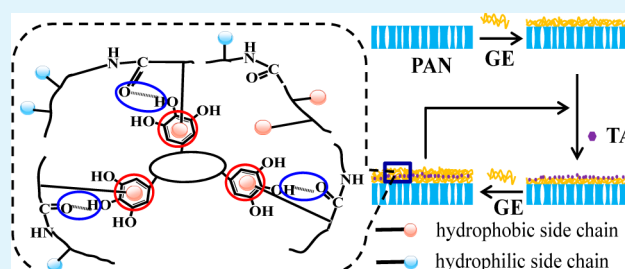
[†]Key Laboratory for Green Chemical Technology of Ministry of Education, School of Chemical Engineering and Technology, Tianjin University, Tianjin 300072, China

[‡]Collaborative Innovation Center of Chemical Science and Engineering (Tianjin), Tianjin 300072, China

[§]Key Laboratory of Nuclear Radiation and Nuclear Energy Technology, Institute of High Energy Physics, Chinese Academy of Sciences, Beijing 100049, China

ABSTRACT: A novel and facile layer-by-layer (LbL) self-assembly process driven by hydrophobic interaction and then reinforced by hydrogen bond was developed to prepare ultrathin membranes. Gelatin (GE) and tannic acid (TA) were alternately deposited on polyacrylonitrile (PAN) ultrafiltration membranes to obtain GE/TA membranes. The required number of deposition cycles for acceptable permselectivity of membrane was greatly reduced compared with that of the traditional LbL self-assembly process and could be ascribed to the rapid growth of membrane thickness and the integrity of the innermost gelatin layer. Higher surface hydrophilicity and more appropriate free volume characteristics were obtained for GE/TA multilayer membranes compared with pristine gelatin membrane. Moreover, the GE/TA multilayer membrane exhibited improved stability even at high water content of 30 wt %. The membrane separation experiments with pervaporation dehydration of ethanol aqueous solution as a model system demonstrated the GE/TA multilayer membrane achieved higher water permselectivity than the pristine gelatin membrane. High operation stability was acquired in the long-term membrane separation test.

KEYWORDS: gelatin/tannic acid, layer-by-layer self-assembly, hydrophobic interaction, hydrogen bond, ultrathin membranes



INTRODUCTION

As a facile method to prepare ultrathin films with tunable thickness, composition, structure, and permeability, layer-by-layer (LbL) self-assembly has received considerable research attention and exhibited prospective applications in realms such as membrane-based separation,^{1,2} drug delivery,^{3,4} biosensors,⁵ and microreactors.^{6,7} The most deeply studied driving force for LbL self-assembly is the electrostatic interaction between oppositely charged species (mainly polyelectrolytes).^{8,9} In each assembly step, a polyelectrolyte layer is adsorbed on the charged substrate and reverses the surface charge so that in the next assembly step a polyelectrolyte layer with opposite charge can be adsorbed.¹⁰ With the development of LbL self-assembly technique, diverse functions and properties are often demanded for multilayer films, which require a broader range of components beyond charged species. As a result, constructing multilayer films on the basis of non-electrostatic interactions such as hydrophobic interaction,¹¹ hydrogen bond,^{12,13} and metal–ligand coordination^{6,9} has gained more and more attention.⁸

Hydrophobic interaction refers to the interaction formed between hydrophobic groups in an aqueous environment under enthalpy effect and entropy effect, which makes the hydro-

phobic groups cluster to reduce their exposure to water molecules. Several researches have been carried out to investigate the functions of hydrophobic interaction in LbL self-assembly.^{14–17} Based on the experimental data and theoretical models, Kotov¹⁵ confirmed that hydrophobic interaction was one of the decisive factors for forming polyelectrolyte multilayers. Furthermore, hydrophobic interaction can promote the assembly of weak polyelectrolytes and increase the growth rate of film thickness.¹⁶ Nevertheless, hydrophobic interaction was often studied as a subsidiary of electrostatic attraction in most researches, and the LbL self-assembly with hydrophobic interaction as the main driving force was scarcely reported.

Tannic acid (TA) is a kind of natural polyphenol, which can bind with proteins through the bifunctions of hydrophobic interaction and hydrogen bond in “hand-glove” reaction mode.¹⁸ First, driven by hydrophobic interactions, tannic acid enters into the hydrophobic pocket formed by the side chains of hydrophobic amino acids on protein. Then, the phenolic

Received: September 28, 2013

Accepted: November 27, 2013

Published: November 27, 2013

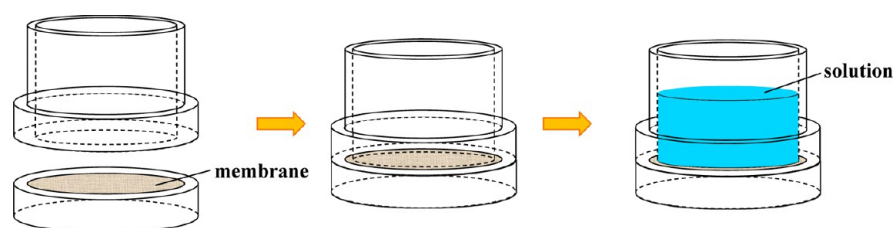


Figure 1. Schematic diagram of the device utilized for membrane fabrication.

hydroxyl groups on tannic acid bind with polar groups on protein chains through hydrogen bonds.^{18,19} It has been revealed that proline-rich protein is more favorable for interacting with tannic acid due to their propensity to form hydrophobic interactions.^{20,21} Gelatin (GE) is a natural protein rich in proline and 4-hydroxyproline,²² which can form strong and multiple interactions with tannic acid and even precipitate when blending with tannic acid. As a polyampholyte, gelatin is an attractive polymer due to its high hydrophilicity, excellent film-forming ability, and wide applications in tissue engineering,²³ drug delivery,²⁴ and membrane-based separation.²⁵

In this study, gelatin and tannic acid were utilized to fabricate ultrathin multilayer membrane on polyacrylonitrile (PAN) ultrafiltration membrane via LbL self-assembly driven by hydrophobic interaction and then reinforced by hydrogen bond. It was envisioned that the multiple interactions and the numerous binding sites could render membranes high stability. The hydrophilicity and structure of the multilayer membranes were extensively characterized. A series of separation experiments were carried out using pervaporation dehydration of ethanol aqueous solution as a model system to investigate the effect of bilayer number and water content in feed solution on the separation performance of multilayer membranes. The operation stability of multilayer membrane was also testified in a long-term membrane separation experiment.

MATERIALS AND METHODS

Materials. Gelatin from porcine skin (Type A, Bloom 300) was supplied by Sigma-Aldrich (U.S.A.). The flat-sheet polyacrylonitrile (PAN) ultrafiltration membrane with a molecular weight cut-off of 100 000 was received from Shanghai MegaVision Membrane Engineering & Technology Co. Ltd. (Shanghai, China). Hydrochloric acid (36–38 wt %) was purchased from Tianjin Kewei Ltd. (Tianjin, China). Ethanol (≥ 99.7 wt %) and tannic acid (MW 1701.2 Da) were received from Tianjin Guangfu Fine Chemical Research Institute (Tianjin, China). All the reagents were of analytical grade and used without further purification. Deionized water was used throughout the experiments.

Preparation of GE/TA Multilayer Membranes. The multilayer membranes were prepared via LbL self-assembly. First, the PAN ultrafiltration membranes (10 cm \times 10 cm) were soaked in deionized water for 2 days to remove glycerin from the surfaces and then fully dried. Meanwhile, gelatin and tannic acid were dissolved in water with concentration of 2.5 mg/mL and then acidified to pH 4.0 utilizing 1 M HCl solution.

In order to avoid the deposition of gelatin and tannic acid on the polyester back side of PAN membrane, a single-side coated approach was employed in the LbL self-assembly process.^{26,27} The schematic diagram of the device utilized for membrane fabrication was shown in Figure 1. The PAN membrane was placed between the two parts of the device, and meanwhile, the two parts were fixed with a clamp to achieve a good sealing. The following steps were performed to deposit gelatin and tannic acid alternately (Figure 2). (a) Gelatin solution was poured into the device and kept still for 5 min. After that, the membrane was dried at room temperature without rinse. (b) Tannic

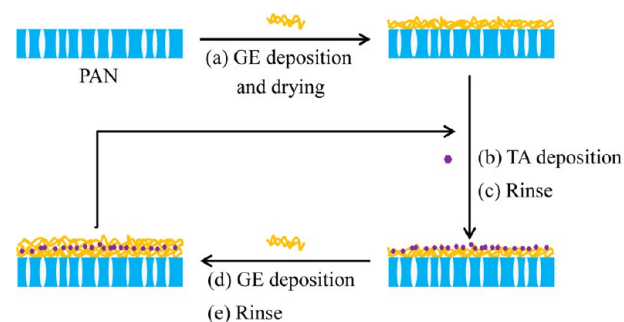


Figure 2. Schematic representation of the fabrication process of multilayer membranes.

acid solution was poured into the device and kept still for 5 min. (c) The membrane was rinsed with HCl solution (pH = 4.0) three times. (d) Gelatin solution was poured into the device and kept still for 5 min. (e) The membrane was rinsed with HCl solution (pH = 4.0) three times. Steps (b–e) were repeated up to the pre-determined times. Subsequently, the membrane was taken out and dried at room temperature. It should be pointed out that it was merely the first cycle of GE deposition conducted without rinsing process, while all the subsequent deposition steps of TA and GE were followed by rinsing processes. All the membranes possessed a gelatin innermost layer, because tannic acid will infiltrate into the nanopores of PAN membrane when being employed as the innermost layer due to its small molecular size. In addition, gelatin was chosen as the outermost layer for all the membrane considering the considerable loss of tannic acid on the membrane surface. The resultant membranes were designated as (GE/TA)_X, where X represented the bilayer number of GE/TA, varying from 0.5 to 5.5. Thereinto, (GE/TA)_{0.5} referred to the membrane just with one gelatin layer. For comparison, gelatin control membrane possessing the similar thickness with (GE/TA)_{5.5} membrane was prepared via dip-coating method using the device in Figure 1 (named as GE).

Membrane Characterizations. The morphology of membrane surface was observed by field emission scanning electron microscope (FESEM) (Nanosem 430) and atomic force microscope (AFM) (CSPM 5000), respectively. The cross-section image of membrane was also obtained by FESEM to measure the thickness of the active layer. At least 10 measurements were taken and averaged for each membrane. The surface hydrophilicity of membrane was evaluated by measuring the static water contact angle at room temperature by a contact angle goniometer (JC2000C Contact Angle Meter). Each membrane should be measured at least six times at different locations of the surface and average data was taken as the final result. Fourier transform infrared (FT-IR) spectra of the membranes in the range 4000–500 cm^{-1} were recorded on a BRUKER Vertex 70 FT-IR spectrometer equipped with a horizontal attenuated total reflectance accessory. Measurements of positron annihilation spectroscopy (PAS) using one high-purity Ge detector were taken in a ²²Na slow positron beamline at room temperature to probe the free volume characteristic of membranes. The positrons implanted into the membrane will annihilate upon encountering electrons in membrane, and release γ photons centered at 511 keV during this process. The distribution of γ photon counts at different photon energies represents the information of cavities in the locations where positrons annihilate. The energy of

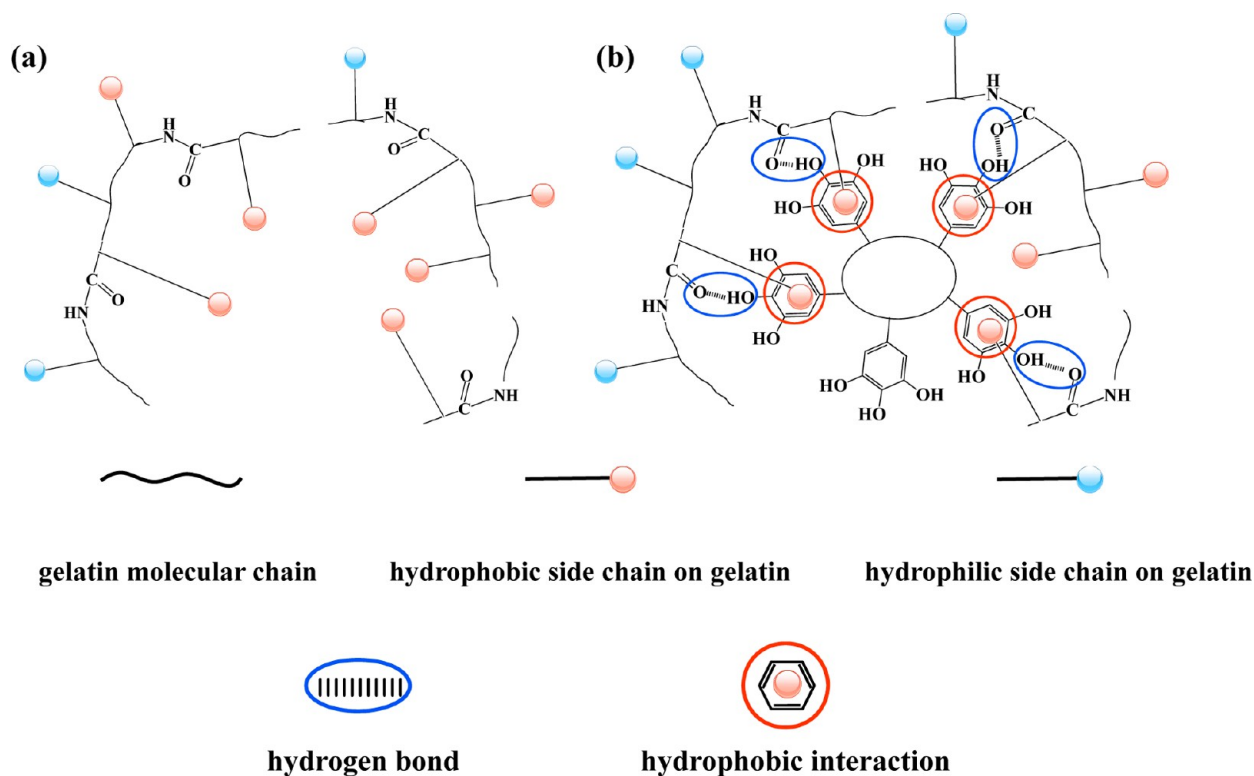


Figure 3. Schematic presentation of the hydrophobic pocket of gelatin (a) with and (b) without tannic acid.

the implanted positrons could be continuously varied in the range of 0.18–20 keV, which corresponds to different positron implantation depths. Therefore, the free volume properties at various depths of the membrane can be acquired by implanting positrons with different energies into membranes and detecting the released γ photons.

Membrane Separation Experiments. GE is a hydrophilic polymer and has been utilized in many water-related membrane processes such as pervaporation dehydration, gas dehumidification, and ultrafiltration for water treatment. Pervaporation is an important membrane process for the separation of liquid mixture with the advantages of high efficiency, environment-benign, energy-saving, and easy operation. In this study, the pervaporation dehydration of ethanol aqueous solution was chosen as the model system to evaluate the separation performance of GE/TA multilayer membranes.

Pervaporation experiments were conducted on the same equipment as reported previously.²⁵ The effective membrane area in contact with feed was 25.6 cm², and the permeate side of the membrane was kept at low pressure (below 0.3 kPa) using a vacuum pump, while the flow rate of feed was controlled at 60 L/h. After the steady state was reached (about 1 h after start-up), the permeate was collected in the cold trap immersed in liquid nitrogen and taken out at fixed intervals. The weight of the permeate solution was measured with an analytical balance. The compositions of feed and permeate solutions were analyzed by gas chromatography (Agilent4890, U.S.A.) equipped with a thermal conductivity detector (TCD) and a column packed with GDX103 (Tianjin Chemical Reagent Co., China). The separation performance of membrane was evaluated by permeation flux (J , g/(m² h)), separation factor (α), and pervaporation separation index (PSI) calculated via the following equations:

$$J = \frac{Q}{At} \quad (1)$$

$$\alpha = \frac{P_W/P_E}{F_W/F_E} \quad (2)$$

$$\text{PSI} = J(\alpha - 1) \quad (3)$$

where Q is the mass of permeate (g) collected during a time interval of t (h) and A is the effective membrane area in contact with the feed (m²). P and F represent the mass fractions of water (with the subscript W) or ethanol (with the subscript E) in the permeate and feed solutions, respectively.

In addition, the permeance of individual components ($(P/l)_i$, GPU) (1 GPU = 7.501×10^{-12} m³ (STP)/(m² s Pa)) and selectivity (β) were calculated by the following equations:²⁸

$$(P/l)_i = \frac{J_i}{P_{i0} - P_{i1}} = \frac{J_i}{\gamma_{i0} x_{i0} p_{i0}^{\text{sat}} - P_{i1}} \quad (4)$$

$$\beta = \frac{(P/l)_W}{(P/l)_E} \quad (5)$$

where J_i is the permeation flux of component i (g/(m² h)), l is the thickness of membrane (m), p_{i0} and p_{i1} are the partial pressures of component i in the feed side and permeate side (Pa), and p_{i1} can be calculated approximately as 0 for the high vacuum degree in the permeate side. γ_{i0} and x_{i0} are the activity coefficient and mole fraction of component i in the feed liquid, respectively. p_{i0}^{sat} is the saturated vapor pressure of pure component i at operation temperature (Pa). The permeation flux of water and ethanol should be transformed into the volumes under standard temperature and pressure (STP): 1 kg of water vapor at STP = 1.245 m³ (STP), 1 kg of ethanol vapor at STP = 0.487 m³ (STP).²⁹

RESULTS AND DISCUSSION

Formation of the Multiple Interactions between Gelatin and Tannic acid. The interactions between protein and polyphenol have been investigated via experiment and molecular modeling approaches in previous studies.^{30,31} On this basis, we proposed the possible model of interactions between gelatin (protein) and tannic acid (polyphenol) during the LbL self-assembly process (as shown in Figure 3). Gelatin is comprised of 18 kinds of amino acids such as proline, 4-hydroxyproline, alanine, arginine, phenylalanine, and glycine.

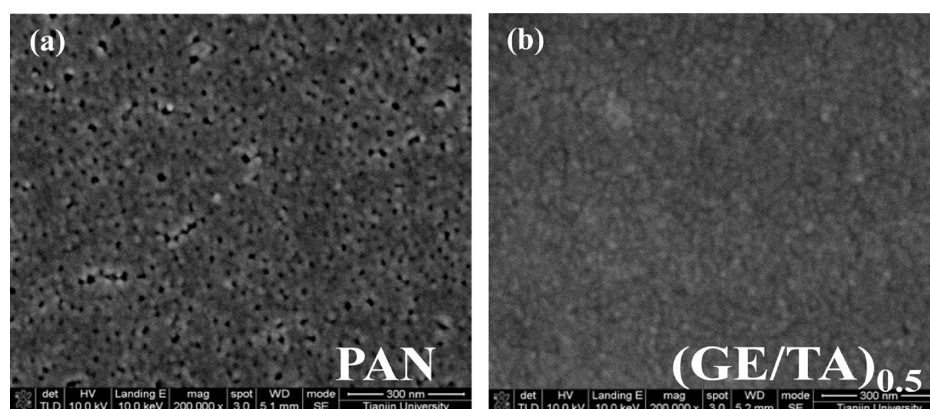


Figure 4. SEM images of the surface morphologies of (a) PAN membrane and (b) (GE/TA)_{0.5} membrane.

Table 1. Surface Roughness of GE/TA Multilayer Membranes with Different Bilayer Numbers

membrane	(GE/TA) _{0.5}	(GE/TA) ₁	(GE/TA) _{1.5}	(GE/TA) ₃	(GE/TA) _{3.5}	(GE/TA) ₅	(GE/TA) _{5.5}
S_q (nm)	2.3	3.5	2.2	4.1	2.1	6.1	2.4

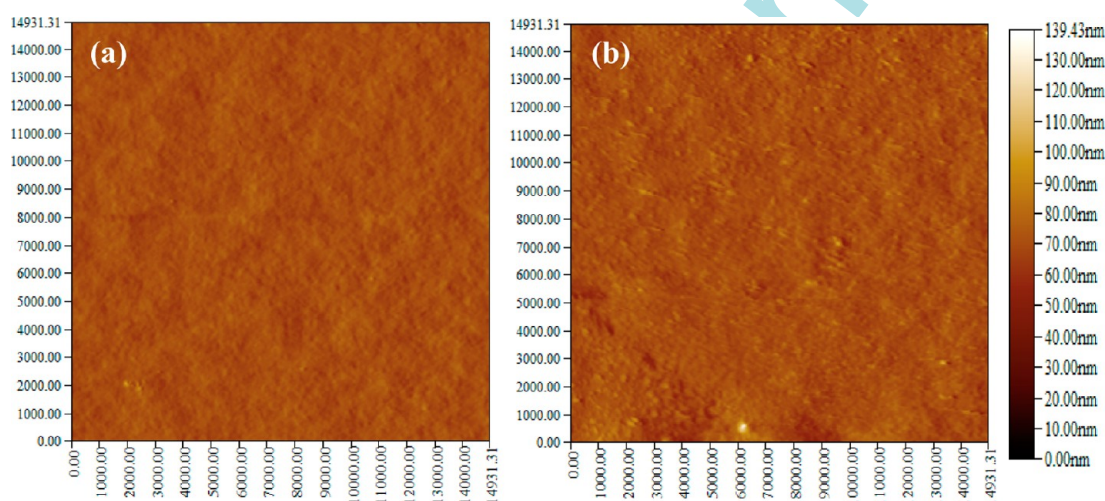


Figure 5. AFM surface topographic images of membranes: (a) (GE/TA)_{0.5} membrane, (b) (GE/TA)₃ membrane.

The hydrophobic amino acid side chains on gelatin such as aromatic ring, pyrrolidine ring, and aliphatic chain are prone to concentrating to form a hydrophobic pocket (Figure 3a).³² Even though the exterior of the hydrophobic pocket comprises of abundant hydrophilic amino acid side chains such as amino group and carboxyl group, there are still some hydrophobic groups on it. In the presence of tannic acid, the aromatic rings of galloyl units on tannic acid attract the hydrophobic groups on gelatin, and then, hydrophobic interactions were formed, thus generating the complex structure of GE and TA. Subsequently, abundant hydrogen bonds are formed between phenolic hydroxyl groups on tannic acid and carbonyl groups on gelatin molecular chains with phenolic hydroxyl groups acting as H donors and carbonyl groups acting as H acceptors,³³ hence stabilizing the complex structure of GE and TA (Figure 3b).^{18,19,34} In that case, more hydrophobic groups are attracted into the hydrophobic pocket due to the attraction of tannic acid. Consequently, the amount of the hydrophobic groups on the exterior of hydrophobic pocket decreases significantly.

Surface Morphology of GE/TA Multilayer Membranes.

The surface morphology of PAN membrane and (GE/TA)_{0.5}

membrane was characterized by FESEM. There were abundant nanopores distributing homogeneously on PAN membrane surface (Figure 4a). After the deposition of the first gelatin layer, no apparent nanopores were observed on the membrane surface (Figure 4b), confirming the complete coverage for the nanopores. Meanwhile, the surface morphology of GE/TA multilayer membranes with different bilayer numbers was characterized by AFM. The corresponding membrane surface roughness S_q was measured via a program in the AFM image processing toolbox and listed in Table 1. It should be pointed out that the S_q value of the PAN membrane was unavailable due to the nanopores on the membrane surface, which made the membrane surface roughness beyond the detection limit of AFM. After the deposition of first layer, the (GE/TA)_{0.5} membrane possessed a smooth surface (as shown in Figure 5a) with a surface roughness of 2.3 nm, further confirming the complete coverage for PAN membrane. The reason was that the first gelatin layer had not been rinsed with HCl solution, and thus, the amount of gelatin deposited on PAN membrane was much larger than that in the traditional LbL assembly process, forming an integral gelatin layer. In comparison, the nanopores on the substrate need a large number of bilayers to

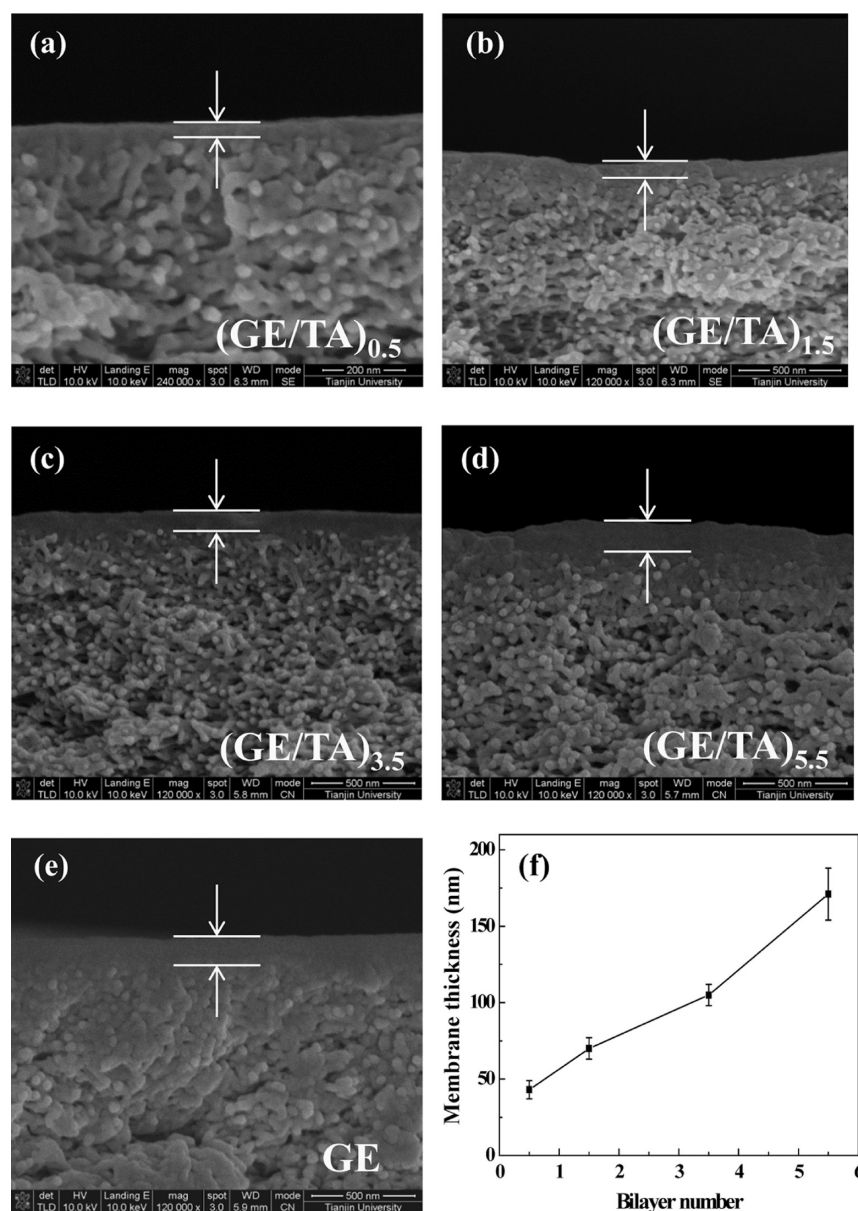


Figure 6. SEM images of the cross-section morphologies of (a) (GE/TA)_{0.5} membrane, (b) (GE/TA)_{1.5} membrane, (c) (GE/TA)_{3.5} membrane, (d) (GE/TA)_{5.5} membrane, (e) GE membrane, and (f) variation of thickness with the bilayer number of GE/TA multilayer membranes.

be fully covered and form a defect-free layer in the traditional LbL assembly process.³⁵

It could be observed from Table 1 that all the membranes possessing a tannic acid outermost layer exhibited higher surface roughness than membranes with a gelatin outermost layer. Figure 5b showed that there were abundant small gibbositities distributing homogeneously on the tannic acid outermost layer, which was caused by the self-association of tannic acid molecules through the π - π interaction between aromatic rings.²⁰

Thickness of GE/TA Multilayer Membranes. The cross-section images of GE/TA multilayer membranes and GE membrane were characterized by FESEM to observe the membrane morphology and measure the thickness of the active layer. It was shown in Figure 6a–e that there was no apparent boundary between the active layer and the support layer, which could be ascribed to the infiltration of coating solution into the nanopores of support layer. Figure 6f showed that the

membrane thickness exhibited a rapid growth^{12,13} and increased from 43 nm to 171 nm with the bilayer number increasing from 0.5 to 5.5. A similar result was also obtained in the LbL self-assembly of epigallocatechin gallate (EGCG) with gelatin (Type A).³⁶ A common explanation for the rapid growth of membrane thickness is the “in-and-out” diffusion model. Some molecules involved in the assembly process may not only be absorbed on the film surface but also diffuse into the interior of the film, which can diffuse out of the film in the subsequent deposition step, and then adsorb more molecules on the film surface.^{10,37,38} The rapid growth of membrane thickness indicated the multi-molecular layer deposition of gelatin and tannic acid in each cycle. In the traditional LbL self-assembly process, at least 50–60 deposition cycles are required to achieve satisfactory permselectivity of membrane, which makes the LbL self-assembly process time-consuming.³⁵ In order to simplify the LbL procedure, pressure enhanced (dynamic deposition)³⁹ and electric field enhanced⁴⁰ strategies

have been employed to increase the thickness and compactness of deposited layers, and then reduce the deposition cycles to less than 10. In this study, the integral innermost gelatin layer and the rapid growth of membrane thickness greatly reduced the required deposition cycles without introducing the external forces, thus greatly simplifying the membrane fabrication procedure. It should be noted that the membrane thickness was lower than most of the current membranes for separation, which was favorable for obtaining low mass transfer resistance and high permeation flux. Additionally, the thickness of GE membrane was 163 nm, close to that of (GE/TA)_{5,5} membrane. Therefore, the performance difference between these two membranes can be entirely attributed to their inherent physical and chemical properties.

Hydrophilicity of GE/TA Multilayer Membranes. The hydrophilicity of the membrane surfaces with different bilayer numbers was evaluated by measuring the static contact angle with water as probe liquid. It was shown in Figure 7 that the

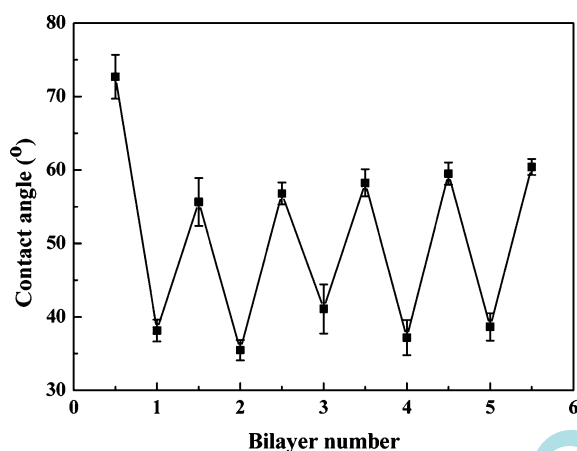


Figure 7. Water contact angles on the surfaces of GE/TA multilayer membranes with different bilayer numbers.

first gelatin layer ((GE/TA)_{0,5} membrane) exhibited a contact angle of 73°, while the other gelatin layers possessed contact angles in the range of 56–60°, demonstrating the increased hydrophilicity of gelatin after self-assembly with tannic acid. The similar variation tendency of hydrophilicity was also reported in literatures with different proteins.⁴¹ The reason was that the hydrophobic groups of tannic acid (such as aromatic ring) interacted with the hydrophobic groups of gelatin (such as the side chains of alanine, valine, leucine, and proline) by forming hydrophobic interactions, leading to the decrease of hydrophobic groups exposed on membrane surface and the consequent increase of hydrophilicity.^{41,42} The GE membrane possessed the same contact angle with (GE/TA)_{0,5} membrane for the identical composition of the two membranes. In addition, tannic acid layers displayed notably higher hydrophilicity (with contact angles around 40°) than gelatin layers due to the abundant hydroxyl groups on tannic acid molecules and the higher surface roughness of tannic acid layers compared with gelatin layers. The alternate variation of contact angles confirmed the LbL self-assembly process of gelatin and tannic acid.

Chemical and Physical Structure of GE/TA Multilayer Membranes. The FT-IR spectra of (GE/TA)_{5,5} and GE membranes are depicted in Figure 8. The characteristic peak around 3300 cm⁻¹ in the spectrum of GE membrane could be

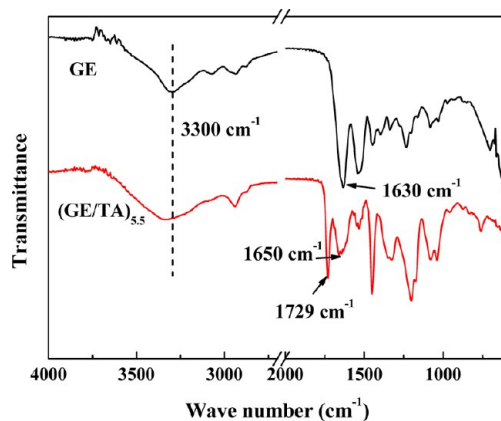


Figure 8. FT-IR spectra of (GE/TA)_{5,5} and GE membranes.

ascribed to the stretching vibration of –OH and –NH₂. After assembling gelatin with tannic acid, the peak was strengthened and broadened due to the abundant phenolic hydroxyl groups on tannic acid. The characteristic peak at 1729 cm⁻¹ in the spectrum of (GE/TA)_{5,5} membrane corresponded to the stretching vibration of C=O in ester group within a conjugation system (the conjugation system between aromatic ring and ester carbonyl group on tannic acid molecule), confirming the successful introduction of tannic acid. Compared the spectrum of (GE/TA)_{5,5} membrane with that of GE membrane, it appeared that the absorption peak of the carbonyl in amide bond shifted from 1630 cm⁻¹ to 1650 cm⁻¹, verifying the existence of hydrogen bonds between gelatin and tannic acid.⁴³

To characterize the microstructure of (GE/TA)_{5,5} and GE membranes, as well as establish the correlation between membrane microstructure and separation performance, the positron annihilation Doppler broadening energy spectra were obtained and described with *S* parameter as a function of positron energy. The *S* parameter is defined as the ratio of the photon annihilation count within the range of 510.24–511.76 keV to that within the range of 504.2–517.8 keV. A decrease in the *S* parameter suggests that the size or concentration of the positron trapping cavities decreases, indicating the decreased fractional free volume and increased membrane compactness. The mean implantation depth of positrons with different energy can be calculated utilizing the following empirical equation,⁴⁴

$$R_e = \left(\frac{40}{\rho} \right) E^{1.6} \quad (6)$$

where *R_e* represents the mean implantation depth (nm), *ρ* is the target density (g/cm³), and *E* is the positron energy (keV). According to the density of gelatin and the active layer thickness of membranes, the position of interface between active layer and support layer could be ascertained at the positron energy of 3 keV. The *S*–*E* curves in Figure 9 revealed that the active layer of (GE/TA)_{5,5} membrane possessed more compact structure compared with that of GE membrane. The result could be ascribed to the abundant hydrophobic interaction sites and hydrogen bonds between gelatin and tannic acid, which achieved the cross-linking for gelatin molecules, hindered the mobility of gelatin chains,²² and then decreased the fractional free volume of gelatin membrane. Additionally, the (GE/TA)_{5,5} membrane exhibited an increased

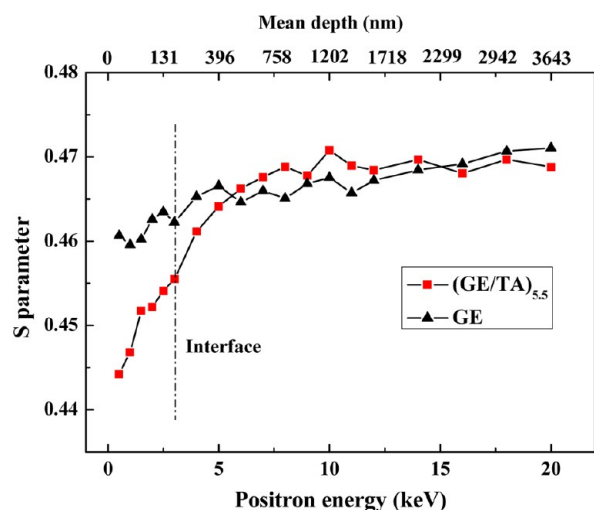


Figure 9. *S* parameter as a function of the positron energy for (GE/TA)_{5.5} and GE membranes.

compactness in the direction from interface to surface. By contrast, the compactness of GE membrane was almost homogeneous in the bulk but with slight increase near the surface.

Pervaporation Performance of GE/TA Multilayer Membranes. The pervaporation performance of GE/TA multilayer membranes and GE membrane was evaluated with 90 wt % ethanol aqueous solution at 350 K and listed in Table 2. It was shown that the (GE/TA)_{0.5} membrane possessed a separation factor of 103 due to the complete coverage for the nanopores on PAN membrane. Because of the integrity of first gelatin layer, together with the rapid growth of membrane thickness, fewer cycles of deposition were adequate to achieve high permselectivity toward water. It was revealed that the separation factor and PSI value increased significantly, while the permeation flux decreased with the bilayer number of GE/TA multilayer membranes varying from 0.5 to 5.5. With the increase of bilayer number, decreased fractional free volume and increased thickness of membrane were obtained, both of which increased the diffusion resistance of permeates, thus leading to the decrease of permeation flux. It could be found in Table 2 that the ethanol flux exhibited a more obvious decrease with the bilayer number increasing than that of water flux due to the larger size of ethanol molecule and the resultant greater influence on its diffusion. As a result, the separation factor displayed remarkable enhancement. It was displayed that the (GE/TA)_{0.5} and GE membranes had similar separation factor because both the active layers of the two membranes were pure gelatin. The GE membrane possessed lower permeation flux than (GE/TA)_{0.5} membrane due to its higher thickness. Except for (GE/TA)_{0.5} membrane, the other GE/TA multilayer membranes exhibited significantly elevated separation factor compared with GE membrane. The mass transport of

molecules through membrane in pervaporation process is based on solution–diffusion theory, and highly-selective separation can be achieved using the differences of permeating molecules in solution property and diffusion property. Compared (GE/TA) membranes with GE membrane, the increased surface hydrophilicity of GE layer favored the preferential solution of water molecules from the water/ethanol mixture. Meanwhile, the free volume characteristic of membrane was tuned to form higher diffusion resistance for the larger ethanol molecules, which increased the diffusion selectivity of water to ethanol. In conclusion, the permselectivity of water was enhanced from both solution and diffusion aspects. The pervaporation performance of (GE/TA)_{5.5} and GE membranes were compared because they had the similar thickness (as shown in Figure 6). It was demonstrated that the (GE/TA)_{5.5} membrane had a 6.1-fold higher separation factor, an only 10% decrease in permeation flux, and the consequent 5.4-fold high PSI value compared with GE membrane.

Figure 10 shows the effect of water content in feed solution (in the range 5–30 wt %) on the pervaporation performance of (GE/TA)_{5.5} and GE membranes at 350 K. It could be observed from Figure 10a that both the permeation flux and water content in permeate of (GE/TA)_{5.5} membrane continued to increase with the water content in feed solution increasing. The high pervaporation performance with the permeation flux of 2696 g/(m² h) and the water content in permeate of 99.4 wt % could be obtained when the water content in feed solution was as high as 30 wt %. The water flux increased significantly, and meanwhile, the ethanol flux decreased slightly with the increase of water content in feed solution. For the GE membrane, a continuously increased water content in permeate was acquired, while the permeation flux increased at first and then decreased at higher water content in feed solution. It was shown in Figure 10b that the ethanol flux and water flux of GE membrane peaked at the points of 15 wt % and 20 wt %, respectively. It is well known that the increased water content in feed solution could elevate the partial pressure of water on the upstream side of membrane, thus leading to the enhancement of driving force for water and the reduction of driving force for ethanol. Meanwhile, the presence of water molecules in membrane would have significant impacts on the membrane structure. In order to analyze the effects of water content in feed solution on pervaporation performance, the permeance and selectivity were calculated and shown in Figure 10, c and d, respectively. It could be observed that the water permeance increased, while the ethanol permeance almost kept constant for (GE/TA)_{5.5} membrane with the water content in feed solution varying from 5 wt % to 30 wt %. The result suggested that the plasticization effect of water molecules swelled the membrane and imparted the membrane with lower water diffusion resistance at higher water content, leading to the significant enhancement of water permeance. Nevertheless, the swelled membrane structure did not promote the diffusion of ethanol. By contrast, both the

Table 2. Pervaporation Performance of GE/TA Multilayer Membranes and GE Membrane

membrane	permeation flux (g/(m ² h))	separation factor	water content in permeate (wt %)	water flux (g/(m ² h))	ethanol flux (g/(m ² h))	PSI (10 ⁵)
(GE/TA) _{0.5}	1756	103	92.0	1615	141	1.81
(GE/TA) _{1.5}	1646	296	97.1	1597	49	4.86
(GE/TA) _{3.5}	1519	491	98.2	1492	27	7.44
(GE/TA) _{5.5}	1336	658	98.7	1318	18	8.78
GE	1490	92	91.1	1357	133	1.36

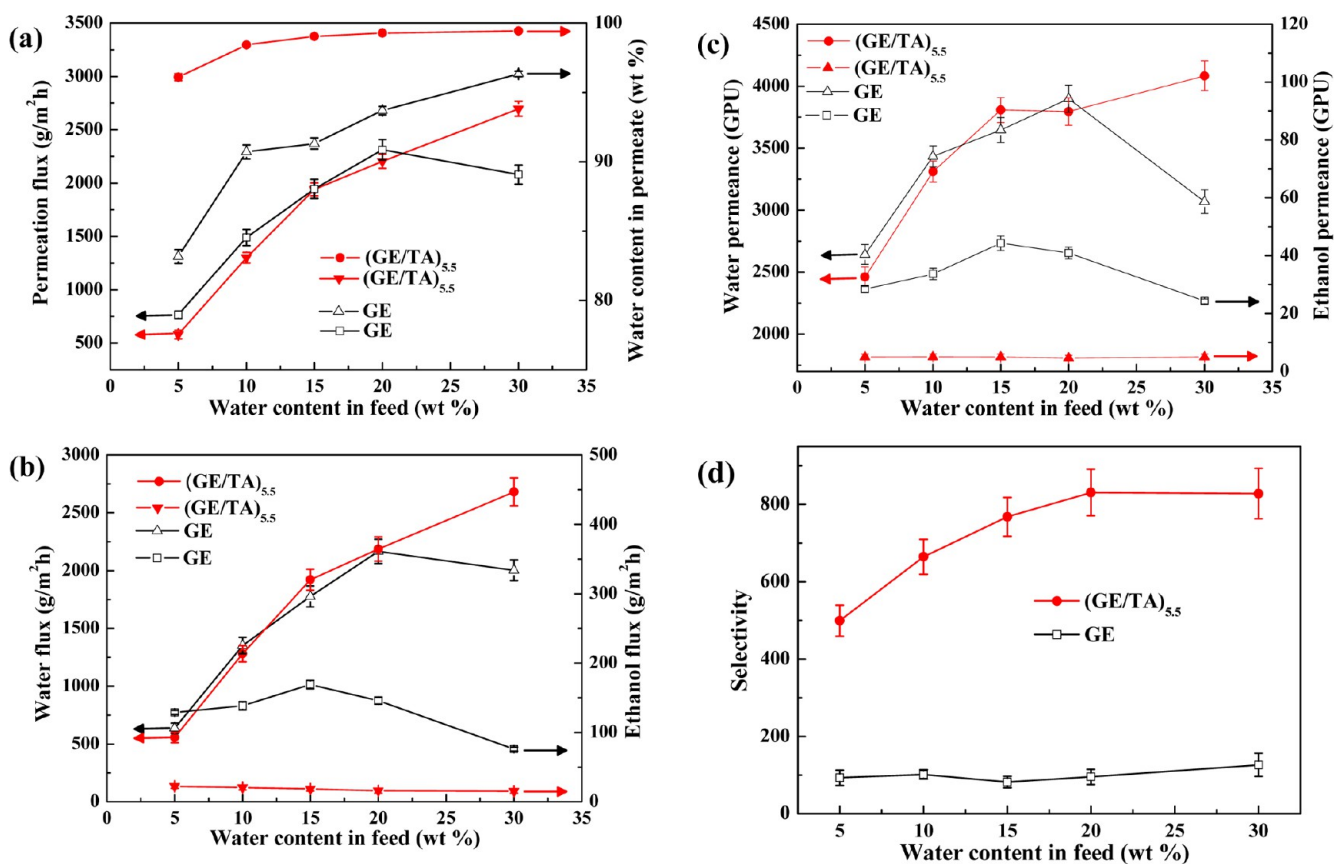


Figure 10. Effect of water content in feed solution on the pervaporation performance of (GE/TA)_{5.5} and GE membranes: (a) permeation flux and water content in permeate; (b) water flux and ethanol flux; (c) water permeance and ethanol permeance; (d) selectivity.

water permeance and ethanol permeance of GE membrane increased at first with the increase of the water content in feed solution, hinting a higher degree of swelling than (GE/TA)_{5.5} membrane, which led to a looser structure favoring the diffusion of water and ethanol. In addition, the ethanol permeance and water permeance of GE membrane began to decline when the water content in feed solution was higher than 15 wt % and 20 wt %, respectively. The possible explanation was that the relaxation of polymer chains played a more important role than the plasticization effect of water in the structure of GE membrane at higher water content in feed solution. It was revealed that higher water content in membrane can facilitate the relaxation process, which can make the membrane structure denser by the configurational rearrangement of polymeric chains.⁴⁵ The above results suggested that the (GE/TA)_{5.5} membrane possessed higher stability than the GE membrane when exposed to feed solutions with higher water content.

In order to investigate the operation stability of the as-prepared multilayer membrane, long-term pervaporation experiment was conducted. Figure 11 showed the pervaporation performance of the (GE/TA)_{5.5} membrane up to 120 h for 90 wt % ethanol aqueous solution at 350 K. During the entire test, the permeation flux decreased slightly at first and then remained almost constant, meanwhile the separation factor fluctuated within a narrow range. The exhibited desirable operation stability confirmed the structural stability of the GE/TA multilayer membrane, and its potential application prospect in pervaporation dehydration process.

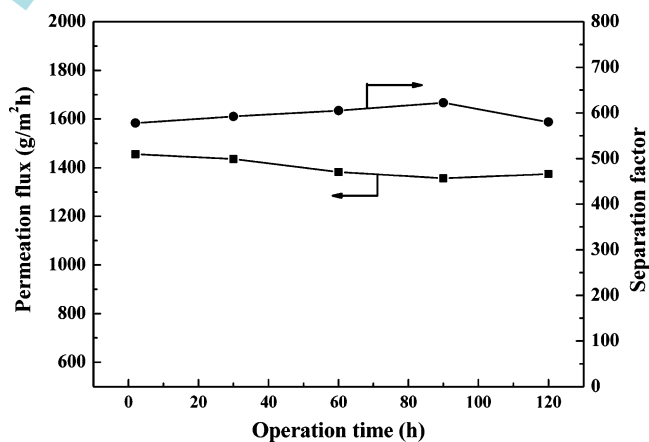


Figure 11. Long-term pervaporation performance of the (GE/TA)_{5.5} membrane.

CONCLUSIONS

A novel and facile approach to fabricating ultrathin membranes was developed via LbL self-assembly process. Gelatin and tannic acid were alternately deposited on PAN ultrafiltration membranes driven by hydrophobic interactions between the aromatic rings on tannic acid and the hydrophobic side chains on gelatin, and then reinforced by numerous hydrogen bonds between phenolic hydroxyl groups on tannic acid and carbonyl groups on gelatin. During the LbL self-assembly process, the rapid growth of membrane thickness and the integral innermost layer were obtained, which contributed to decreasing the required deposition cycles for satisfactory permselectivity of

membrane, thus simplifying the membrane-fabrication procedure. Hydrophobic interaction played the following three roles: (1) enabling LbL self-assembly process; (2) decreasing the hydrophobic groups on membrane surface, and then increasing the hydrophilicity of gelatin membrane; (3) providing sufficient interactions between adjacent layers together with hydrogen bond, then tuning the free volume characteristics and increasing the stability of gelatin membrane. Consequently, the GE/TA multilayer membranes exhibited improved separation performance compared with pristine gelatin membrane. Enhanced operation stability for GE/TA multilayer membranes was also demonstrated with a long-term membrane separation experiment. Considering the wide applicability of protein in biomedical, membrane-based separation and so forth, this type of LbL self-assembly provides a facile and eco-friendly approach to fabricating protein-contained films with high stability, tunable structure and properties.

AUTHOR INFORMATION

Corresponding Author

*Fax: +86 22 2350 0086. Tel: +86 22 2350 0086. E-mail: zhyjiang@tju.edu.cn.

Notes

The authors declare no competing financial interest.

ACKNOWLEDGMENTS

The authors gratefully acknowledge the financial support from the National Science Fund for Distinguished Young Scholars (21125627), the National Natural Science Foundation of China (No. 21306131), Specialized Research Fund for the Doctoral Program of Higher Education (20120032120009), Seed Foundation of Tianjin University, and the Program of Introducing Talents of Discipline to Universities (No. B06006).

REFERENCES

- (1) Yin, M. J.; Qian, J. W.; An, Q. F.; Zhao, Q.; Gui, Z. L.; Li, J. *J. Membr. Sci.* **2010**, *358*, 43–50.
- (2) Li, J.; Zhang, G. J.; Ji, S. L.; Wang, N. X.; An, W. *J. Membr. Sci.* **2012**, *415–416*, 745–757.
- (3) Chen, D. D.; Chen, J.; Wu, M. D.; Tian, H. Y.; Chen, X. S.; Sun, J. *Q. Langmuir* **2013**, *29*, 8328–8334.
- (4) Wu, Z. G.; Wu, Y. J.; He, W. P.; Lin, X. K.; Sun, J. M.; He, Q. *Angew. Chem., Int. Ed.* **2013**, *52*, 7000–7003.
- (5) Yu, C. M.; Wang, Y. D.; Wang, L.; Zhu, Z. K.; Bao, N.; Gu, H. Y. *Colloids Surf., B* **2013**, *103*, 231–237.
- (6) Wang, X. L.; Jiang, Z. Y.; Shi, J. F.; Liang, Y. P.; Zhang, C. H.; Wu, H. *ACS Appl. Mater. Interfaces* **2012**, *4*, 3476–3483.
- (7) Sakr, O. S.; Borchard, G. *Biomacromolecules* **2013**, *14*, 2117–2135.
- (8) Quinn, J. F.; Johnston, A. P. R.; Such, G. K.; Zelikin, A. N.; Caruso, F. *Chem. Soc. Rev.* **2007**, *36*, 707–718.
- (9) Zhang, G. J.; Ruan, Z. G.; Ji, S. L.; Liu, Z. Z. *Langmuir* **2010**, *26*, 4782–4789.
- (10) Li, Y.; Wang, X.; Sun, J. Q. *Chem. Soc. Rev.* **2012**, *41*, 5998–6009.
- (11) Zhou, J.; Wang, B.; Tong, W. J.; Maltseva, E.; Zhang, G.; Krastev, R.; Gao, C. Y.; Möhwald, H.; Shen, J. C. *Colloids Surf., B* **2008**, *62*, 250–257.
- (12) Kozlovskaya, V.; Kharlampieva, E.; Drachuk, I.; Cheng, D.; Tsukruk, V. V. *Soft Matter* **2010**, *6*, 3596–3608.
- (13) Lisunova, M. O.; Drachuk, I.; Shchepelina, O. A.; Anderson, K. D.; Tsukruk, V. V. *Langmuir* **2011**, *27*, 11157–11165.
- (14) Ouyang, X. P.; Deng, Y. H.; Qian, Y.; Zhang, P.; Qiu, X. Q. *Biomacromolecules* **2011**, *12*, 3313–3320.
- (15) Kotov, N. A. *Nanostruct. Mater.* **1999**, *12*, 789–796.
- (16) Li, C.; Zhang, J.; Yang, S.; Li, B. L.; Li, Y. Y.; Zhang, X. Z.; Zhuo, R. X. *Phys. Chem. Chem. Phys.* **2009**, *11*, 8835–8840.
- (17) Guo, X. H.; Zhang, H.; Hu, N. F. *Nanotechnology* **2008**, *19*, 055709.
- (18) Yi, K. J.; Cheng, G. X.; Xing, F. B. *J. Appl. Polym. Sci.* **2006**, *101*, 3125–3130.
- (19) Hagerman, A. E. *ACS Symp. Ser.* **1992**, *506*, 236–247.
- (20) Baxter, N. J.; Lilley, T. H.; Haslam, E.; Williamson, M. P. *Biochemistry* **1997**, *36*, 5566–5577.
- (21) Canon, F.; Paté, F.; Cheynier, V.; Machado, S. M.; Giuliani, A.; Pérez, J.; Durand, D.; Li, J.; Cabane, B. *Langmuir* **2013**, *29*, 1926–1937.
- (22) Peña, C.; Caba, K.; Eceiza, A.; Ruseckaite, R.; Mondragon, I. *Bioresour. Technol.* **2010**, *101*, 6836–6842.
- (23) Mahony, O.; Tsigkou, O.; Ionescu, C.; Minelli, C.; Ling, L.; Hanly, R.; Smith, M. E.; Stevens, M. M.; Jones, J. R. *Adv. Funct. Mater.* **2010**, *20*, 3835–3845.
- (24) Ding, D.; Zhu, Z. S.; Li, R. T.; Li, X. L.; Wu, W.; Jiang, X. Q.; Liu, B. R. *ACS Nano* **2011**, *5*, 2520–2534.
- (25) Zhao, J.; Ma, J.; Chen, J.; Pan, F. S.; Jiang, Z. Y. *Chem. Eng. J.* **2011**, *178*, 1–7.
- (26) Zhu, Z. Q.; Feng, X. S.; Penlidis, A. *Mater. Sci. Eng., C* **2006**, *26*, 1–8.
- (27) Ng, L. Y.; Mohammad, A. W.; Ng, C. Y. *Adv. Colloid Interface Sci.* **2013**, *197–198*, 85–107.
- (28) Baker, R. W.; Wijmans, J. G.; Huang, Y. J. *Membr. Sci.* **2010**, *348*, 346–352.
- (29) Tripathi, B. P.; Kumar, M.; Saxena, A.; Shahi, V. K. *J. Colloid Interface Sci.* **2010**, *346*, 54–60.
- (30) Charlton, A. J.; Haslam, E.; Williamson, M. P. *J. Am. Chem. Soc.* **2002**, *124*, 9899–9905.
- (31) Richard, T.; Vitrac, X.; Merillon, J. M.; Monti, J. P. *Biochim. Biophys. Acta* **2005**, *1726*, 238–243.
- (32) Shi, B.; He, X. Q.; Haslam, E. *J. Am. Leather Chem. Assoc.* **1994**, *89*, 98–104.
- (33) Unal, I. E.; Sukhishvili, S. A. *Macromolecules* **2008**, *41*, 3962–3970.
- (34) Quideau, S.; Deffieux, D.; Casassus, C. D.; Pouységu, L. *Angew. Chem. Int. Ed.* **2011**, *50*, 586–621.
- (35) Krasemann, L.; Toutianoush, A.; Tieke, B. *J. Membr. Sci.* **2001**, *181*, 221–228.
- (36) Shutava, T. G.; Balkundi, S. S.; Lvov, Y. M. *J. Colloid Interface Sci.* **2009**, *330*, 276–283.
- (37) Liu, H. Y.; Hu, N. F. *J. Phys. Chem. B* **2006**, *110*, 14494–14502.
- (38) Richerd, L.; Lavalle, P.; Payan, E.; Shu, X. Z.; Prestwich, G. D.; Stoltz, J. F.; Schaaf, P.; Voegel, J. C.; Picart, C. *Langmuir* **2004**, *20*, 448–458.
- (39) Zhang, G. J.; Wang, N. X.; Song, X.; Ji, S. L.; Liu, Z. Z. *J. Membr. Sci.* **2009**, *338*, 43–50.
- (40) Zhang, P.; Qian, J. W.; An, Q. F.; Liu, X. Q.; Zhao, Q.; Jin, H. T. *J. Membr. Sci.* **2009**, *328*, 141–147.
- (41) Aewsiri, T.; Benjakul, S.; Visessanguan, W.; Wierenga, P. A.; Gruppen, H. *Innovative Food Sci. Emerging Technol.* **2010**, *11*, 712–720.
- (42) Rawel, H. M.; Czajka, D.; Rohn, S.; Kroll, J. *Int. J. Biol. Macromol.* **2001**, *3–4*, 137–150.
- (43) Wang, L. Y.; Wang, Z. Q.; Zhang, X.; Shen, J. C.; Chi, L. F.; Fuchs, H. *Macromol. Rapid Commun.* **1997**, *18*, 509–514.
- (44) Li, B.; Liu, W. P.; Jiang, Z. Y.; Dong, X.; Wang, B. Y.; Zhong, Y. R. *Langmuir* **2009**, *25*, 7368–7374.
- (45) Yeom, C. K.; Jegal, J. G.; Lee, K. H. *J. Appl. Polym. Sci.* **1996**, *62*, 1561–1576.